Elemental diffusion during the droplet epitaxy growth of In(Ga)As/GaAs(001) quantum dots by metal-organic chemical vapor deposition

Z. B. Chen, W. Lei, B. Chen, Y. B. Wang, X. Z. Liao, H. H. Tan, J. Zou, S. P. Ringer, and C. Jagadish

Citation: Applied Physics Letters **104**, 022108 (2014); doi: 10.1063/1.4859915
View online: http://dx.doi.org/10.1063/1.4859915
View Table of Contents: http://scitation.aip.org/content/aip/journal/apl/104/2?ver=pdfcov
Published by the AIP Publishing

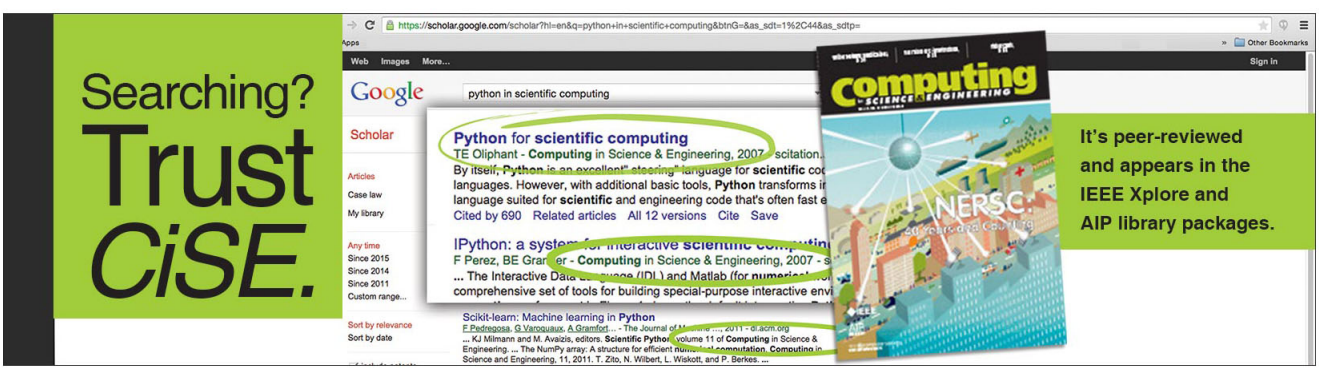

Elemental diffusion during the droplet epitaxy growth of In(Ga)As/GaAs(001) quantum dots by metal-organic chemical vapor deposition

Z. B. Chen,[1] W. Lei,[2] B. Chen,[1] Y. B. Wang,[1] X. Z. Liao,[1,a)] H. H. Tan,[3] J. Zou,[4] S. P. Ringer,[1,5] and C. Jagadish[3]
[1]*School of Aerospace, Mechanical and Mechatronic Engineering, The University of Sydney, Sydney, NSW 2006, Australia*
[2]*School of Electrical, Electronic and Computer Engineering, The University of Western Australia, Perth, WA 6009, Australia*
[3]*Department of Electronic Materials Engineering, Research School of Physics and Engineering, The Australian National University, Canberra, ACT 0200, Australia*
[4]*Materials Engineering and Centre for Microscopy and Microanalysis, The University of Queensland, Brisbane, QLD 4072, Australia*
[5]*Australian Centre for Microscopy and Microanalysis, The University of Sydney, Sydney, NSW 2006, Australia*

(Received 6 September 2013; accepted 15 December 2013; published online 15 January 2014)

Droplet epitaxy is an important method to produce epitaxial semiconductor quantum dots (QDs). Droplet epitaxy of III-V QDs comprises group III elemental droplet deposition and the droplet crystallization through the introduction of group V elements. Here, we report that, in the droplet epitaxy of InAs/GaAs(001) QDs using metal-organic chemical vapor deposition, significant elemental diffusion from the substrate to In droplets occurs, resulting in the formation of In(Ga)As crystals, before As flux is provided. The supply of As flux suppresses the further elemental diffusion from the substrate and promotes surface migration, leading to large island formation with a low island density. © *2014 AIP Publishing LLC*. [http://dx.doi.org/10.1063/1.4859915]

Epitaxial semiconductor quantum dots (QDs) have been widely investigated because of their potential significant electronic and optoelectronic applications.[1–3] The structural parameters of QDs including their shape, size, number density, and composition are of crucial significance in determining the electrical and optical properties of the QDs.[4] To precisely control these microstructure parameters, it is critical to have a thorough understanding of the growth mechanisms of the QDs.[5]

There are two major growth modes used to produce epitaxial QDs—the Stranski-Krastnow (S-K) growth mode[6] and the droplet epitaxy approach.[7] The S-K growth mode has been used to fabricate reliable semiconductor devices in material systems with significant lattice mismatch.[8,9] Here, layer-by-layer growth is followed by island formation to release the strain energy caused by the lattice mismatch between the epilayer and the substrate. It has been reported that the S-K growth of QDs is a very complicated process, which includes atomic interdiffusion between the QDs and the substrate[10–12] and elemental redistribution within QDs.[13] The elemental distribution within the QDs has been shown to affect the QD morphology,[14] and the compositional evolution in InGaAs/GaAs QDs[15] and Ge/Si QDs[14,16] grown using the S-K mode have been reported.

The droplet epitaxy approach can be used in systems with or without lattice mismatch,[17–20] and involves two steps: (i) deposition of droplets of an element and (ii) crystallization of these droplets through the reaction of the droplets with another element. For the droplet epitaxy of III-V semiconductor QDs, liquid droplets of group III elements are first introduced on the substrate and then exposed to group V elements. The detailed mechanisms of droplet epitaxy growth are much less explored than those of the S-K growth mode. In this Letter, we present a detailed microscopy-based-investigation of the composition and morphology of In(Ga)As/GaAs QDs grown by droplet epitaxy in a metal-organic chemical vapor deposition (MOCVD) system. Our experimental results demonstrate that droplet epitaxy QD growth is a complicated process and we suggest a modified mechanism for droplet epitaxy growth.

The In droplet and InAs QD samples for this study were grown on semi-insulating GaAs(001) substrates in a horizontal flow MOCVD reactor (AIX200/4) at a pressure of 100 millibars. Trimethylindium, trimethylgallium, and AsH_3 were used as the precursors and ultra-high purity H_2 as the carrier gas. A 200 nm GaAs buffer layer was first deposited at 650 °C, followed by reducing the temperature to 500 °C with AsH_3 flowing. When the temperature reached 500 °C, a 10 s interruption was introduced, whereby AsH_3 was removed from the reactor to eliminate the influence of AsH_3 on subsequent deposition of In droplets. Afterwards, "two monolayer" of In droplets (the In amount used to grow two monolayer InAs in normal epitaxy under the same growth conditions) were deposited. Sample $QD_{In\text{-}only}$ refers to the sample immediately cooled to room temperature without exposure to AsH_3 flux after In droplet deposition, while the temperature in sample QD_{In+8s} was maintained for an additional 8 s after In deposition and without exposure to AsH_3 flux. Sample QD_{InAs} was prepared by immediate exposure of In droplets to the AsH_3 flow (3.0×10^{-4} mol/min) for 8 s after In droplet deposition.

Plan-view and cross-sectional transmission electron microscopy (TEM) specimens were prepared using a Gatan precision ion polishing system with Ar^+ energy of 3 keV. The

a)Electronic mail: xiaozhou.liao@sydney.edu.au. Tel.: +61 2 9351 2348.

surface morphology of the three samples was characterized using a Zeiss Ultra+ scanning electron microscope (SEM) operating at 5 kV. Structural characterization using high-resolution TEM and selected area electron diffraction (SAED) was carried out in a JEM-3000F TEM operating at 300 kV. Quantitative compositional analysis was conducted using energy dispersive x-ray spectroscopy (EDXS) in a JEM-2200 TEM operating at 200 kV and the ESPRIT software. The electron probe size for the EDXS was 1 nm. The EDXS data were collected and averaged from 10 QDs for each specimen. The error bar for each EDXS datum indicates the highest and lowest experimental results.

Figure 1(a) shows a typical $\langle 110 \rangle_{\text{substrate}}$ cross-sectional high-resolution TEM image of an In droplet in sample $QD_{\text{In-only}}$. The image suggests that the island was epitaxially grown on the substrate surface with the same atomic arrangement as that of the GaAs substrate and with a slightly larger lattice parameter. Misfit dislocations, indicated by white arrowheads, with extra half atomic planes are present at the island/substrate interface. The misfit dislocations are caused by the lattice mismatch. Figure 1(b) shows a combined $\langle 110 \rangle$ cross-sectional SAED pattern recorded from the island and the substrate shown in Fig. 1(a). Two sets of reciprocal space lattices are visible. The one with the strong diffraction spots (marked with "1") is from the substrate, while the one with weak diffraction spots (marked with "2") is from the island. Figure 1(b) further confirms that the island has the same two-dimensional lattice structure as the substrate but with a larger lattice parameter when observed along the $\langle 110 \rangle$ direction.

Figure 1(c) shows a typical [001] plan-view image of a relaxed droplet island and the surrounding substrate area. The two-dimensional Moiré fringes shown in Figure 1(c) are caused by the lattice mismatch between the island and the substrate. Fig. 1(d) presents a combined [001] plan-view SAED pattern recorded from the region shown in Fig. 1(c). The combined messages obtained from Figs. 1(b) and 1(d) provide a complete three-dimensional reciprocal structural information demonstrating that the droplet possesses the same lattice structure as the substrate, i.e., face centred cubic lattice or the zinc-blende structure, but with a larger lattice parameter than the substrate. However, pure In possesses a tetragonal crystal structure at room temperature,[21] which is certainly not consistent with the experimental SAED patterns. This suggests that alloying of the In droplet to form InAs or InGaAs island has occurred.

To confirm this hypothesis, EDXS microanalysis was conducted to determine the chemical composition of the droplets in all the three samples. Islands from samples $QD_{\text{In-only}}$, $QD_{\text{In+8s}}$, and QD_{InAs} with base diameters in the range of ~30–60 nm and similar height-to-base diameter ratios of ~1:2.5 were chosen for the EDXS microanalysis. Figure 2(a) presents a typical image of an island from sample $QD_{\text{In-only}}$ for EDXS microanalysis. The black lines A, B, and C indicates the EDXS line scan, from which In, Ga, and As were detected. Because the height and aspect ratio of islands in different samples are different, the horizontal axis in Figs. 2(b) and 2(c) is scaled appropriately such that positions A, B, and C consistently represent positions at the substrate, the island/substrate interface, and the top of islands, respectively. Figure 2(b) presents the ratios of the atomic percentages of As to that of In + Ga at the substrate and different positions on the island in each of the three samples. The As/(In + Ga) ratio remains approximately constant at around 1:1 along the line scan for samples $QD_{\text{In-only}}$ and $QD_{\text{In+8s}}$, indicating that the droplets in these two samples have fully

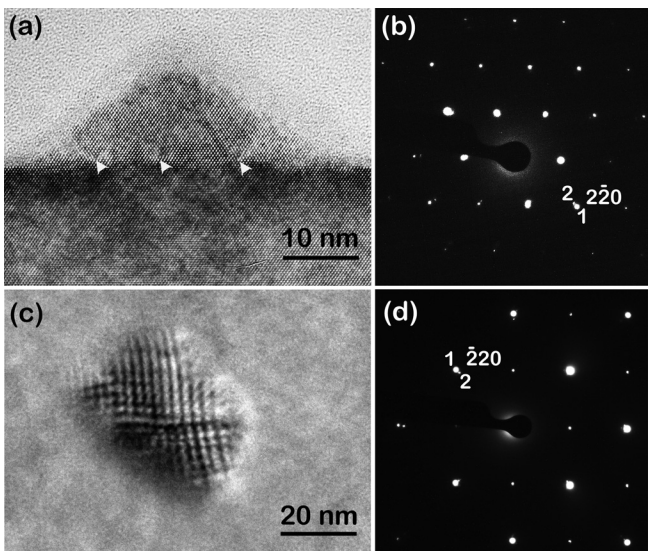

FIG. 1. A $\langle 110 \rangle$ cross-sectional high-resolution TEM image of sample $QD_{\text{In-only}}$. Misfit dislocations at the island/substrate interface are indicated using white arrowheads; (b) a combined SAED pattern from the area shown in (a); (c) a typical [001] bright-field plan-view image of a large island in sample $QD_{\text{In-only}}$; and (d) a corresponding SAED pattern taken from the area shown in (c). Diffraction spots from the substrate and islands in (b) and (d) are indicated by "1" and "2," respectively.

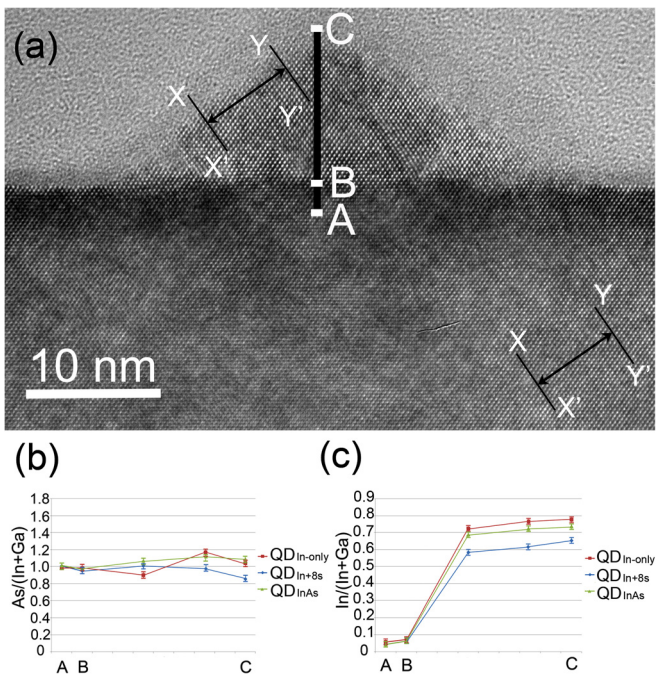

FIG. 2. (a) A $\langle 110 \rangle$ cross-sectional TEM image of a relaxed InGaAs island. The straight lines A, B, and C indicate the positions from which EDXS data were obtained. Point B is immediately below the island/substrate interface. Two groups of parallel lines XX′ and YY′ are drawn to be parallel to a group of {111} planes and to have the distance of 24 {111} planes; (b) the As/(In + Ga) ratio from EDXS data detected along the lines A, B, and C in (a); and (c) the In/(In + Ga) ratio from the EDXS data.

crystallized through As diffusion from the substrate to the droplets, since AsH_3 flow was not introduced in these two samples. Due to the introduction of AsH_3 in the preparation of sample QD_{InAs}, the As/(In + Ga) ratio for this sample was expected to be 1 and this was observed experimentally in Fig. 2(b). Slight deviations of the As/(In + Ga) ratio from exact 1:1 in QDs were caused by the non-equilibrium state of the three samples. Figure 2(c) shows the In/(In + Ga) ratio along the line scan for the three samples. Sample $QD_{In\text{-}only}$ has the highest In/(In + Ga) ratio, while sample QD_{In+8s} has the lowest value. The In/(In + Ga) ratio for sample QD_{InAs} is close to that of sample $QD_{In\text{-}only}$. Note that EDXS measurement from the substrate far away from the island/substrate interface shows that the composition of substrate is exactly GaAs, which confirms the accuracy of our EDXS data. The error bars of EDXS data were measured within ±3% of the mean values, which are smaller than the composition variations among the three samples.

In droplet epitaxy of InAs/GaAs QDs, it was believed that In would remain as a pure liquid droplet before the As flux is introduced to the reaction chamber[22] which will then subsequently result in the crystallization of In to InAs[23] such that the stoichiometry of the resultant islands should be III:V = 1:1.[24] However, a zinc-blende structure was formed in the droplets of samples $QD_{In\text{-}only}$ and QD_{In+8s} prior to admittance of the As flux, and the ratios of As to In + Ga in the droplets were confirmed to be ~1:1 by EDXS analysis in Fig. 2(c). This demonstrates that Ga and As atoms have diffused into the substrate to form crystalline In(Ga)As islands.

Although the presence of As in In droplets prior to the admittance of the As flux has been mentioned previously, it is not clear whether the group V element originates from the substrate or from the contaminated reaction chamber.[25] In our experiment, a clean reaction chamber was used, and AsH_3 was removed after the growth of the GaAs buffer layer. In addition, H_2 was used to flush the chamber. Therefore, the substrate is considered to be the main source of As for samples $QD_{In\text{-}only}$ and QD_{In+8s} due to the fact that a local As environment could be formed directly at the sample surface caused by the out-diffusion of As from the substrate and buffer layer since the temperature is still quite high, even though prior deposition on the liner and suspecter in the reaction chamber may potentially play a role. At the growth temperature of 500 °C and without AsH_3 flow, some Ga-As bonds in the areas around the droplets would tend to break, resulting in As desorption,[26] which then alloys with the pure In droplets. Some excess Ga atoms, resulting from the desorption of As, diffuse into the In droplets (as discussed below). However, most of the Ga remained either on the substrate or diffused into the substrate to form Ga interstitials.[27,28] This would change the stoichiometry of the GaAs substrate in the vicinity of the islands, and this was confirmed by the As/(In + Ga) ratio between A and B of slightly less than 1 (note that the ratio between A and B may be overestimated due to the poor spatial resolution of EDXS at a relatively thick substrate). These SAED and EDXS data indicate that the QD growth by droplet epitaxy is much more complicated than the ideal situation that is often proposed.[23]

According to Vegard's law,[29] the composition in the relaxed islands can be evaluated via a comparison of the lattice parameters between the relaxed islands and the substrate. Lattice parameters were measured using the method demonstrated in Figure 2(a). Two groups of parallel lines XX′ and YY′ with a distance of 24 {111} atomic planes were drawn in the substrate and the island far away from the island/substrate interface. The distances between the two groups of the parallel lines were accurately measured.

Cohen *et al.*[4] reported substantial diffusion of Group III elements (e.g., In or Ga) between the islands and the substrate in III-V QDs grown by droplet epitaxy. However, little has been reported about the details of the diffusion stage. To probe this further, the island compositions of the three samples measured from EDXS and high-resolution TEM images are listed in Table I. The islands in all three samples contain more In than Ga. Although there is a slight discrepancy between the results obtained from EDXS and those from high-resolution TEM, the general trend on the relative atomic percentages of In and Ga in the three samples is the same, i.e., sample $QD_{In\text{-}only}$ has the highest In content (lattice mismatch = 5.8%) and sample QD_{In+8s} has the lowest (lattice mismatch = 4.6%). It is clear that substantial diffusion of As and Ga from the substrate to the islands occurs during the deposition of the In droplets. This diffusion likely includes both bulk and surface diffusion. Bulk diffusion occurs directly underneath the In droplets along the vertical direction, while surface diffusion takes place in the areas around the In droplets. A driving force for Ga diffusion into the islands is the reduction of the overall elastic energy of the system.[30] Indeed, the incorporation of Ga atoms into InAs QDs during the nucleation and growth process under S-K mode has been reported before.[15] In our case, the Ga atoms liberated from the breaking of the Ga-As bonds in the areas underneath/around the droplets at high temperature can diffuse/migrate into the islands to form an alloy. This diffusion/migration process is evidenced by the fact that sample QD_{In+8s} was found to show a larger amount of Ga, suggesting more diffusion of Ga from the substrate to the islands due to the 8 s growth interruption at high temperature without the As flux.

Sample QD_{InAs} was exposed to the As flux for 8 s at 500 °C, while sample QD_{In+8s} remained at the same temperature for 8 s after In deposition without admittance of the As flux. The lower Ga content in the islands in sample QD_{InAs} (compared to sample QD_{In+8s}) indicates that the diffusion of Ga from the substrate to the islands is suppressed by the supply of the As flux. This is because the presence of As adatoms on the surface introduced by the AsH_3 flow stabilizes Ga-As bonds on the substrate surface, leading to the suppression of Ga diffusion to the islands after the deposition of In

TABLE I. Island compositions obtained from high-resolution TEM images and EDXS.

Samples	Lattice-mismatch between islands and substrate (%)	Composition deduced from lattice mismatch	Composition from EDXS
$QD_{In\text{-}only}$	5.8	$In_{0.80}Ga_{0.20}As$	$In_{0.75}Ga_{0.25}As$
QD_{In+8s}	4.6	$In_{0.64}Ga_{0.36}As$	$In_{0.60}Ga_{0.40}As$
QD_{InAs}	5.7	$In_{0.79}Ga_{0.21}As$	$In_{0.72}Ga_{0.28}As$

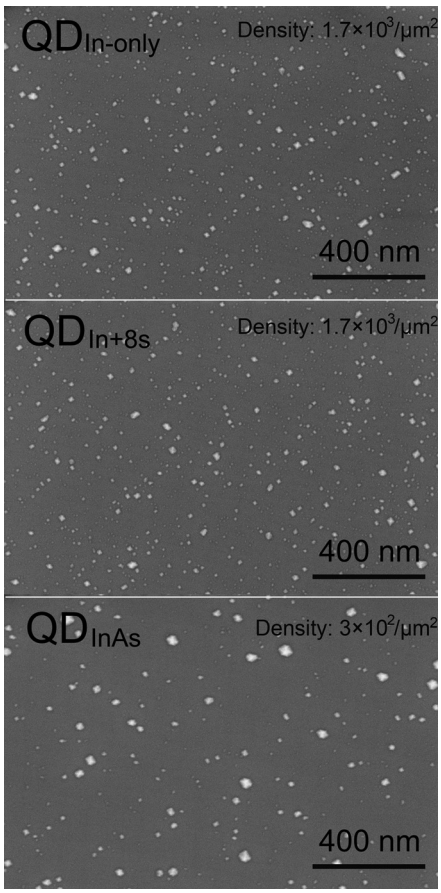

FIG. 3. SEM images of the surfaces of samples $QD_{In\text{-}only}$, QD_{In+8s} and QD_{InAs}.

droplets. Note that the Ga content in the islands in sample $QD_{In\text{-}only}$ is also lower than that in sample QD_{In+8s} because there was not enough time for Ga diffusion to islands in sample $QD_{In\text{-}only}$.

Although the evolution of size and density of S–K InAs QDs under As ambient has been widely studied,[31,32] little is known about the effect of As flux on the surface morphology evolution of InAs QDs grown by droplet epitaxy. Figure 3 shows plan-view SEM images of the three samples. There is no morphological difference between sample $QD_{In\text{-}only}$ and sample QD_{In+8s}. A bimodal size distribution with ranges of 10–20 nm and 30–40 nm in diameter and with a density of $\sim 1.7 \times 10^3/\mu m^2$ are measured for the QDs in samples $QD_{In\text{-}only}$ and QD_{In+8s}. Islands with diameters larger than $\sim$20 nm account for less than 20% of all islands in both samples.

Interestingly, a remarkably different morphology is observed in sample QD_{InAs} with a low QD density of $\sim 3 \times 10^2/\mu m^2$ and a larger size distribution of $\sim$10–70 nm. Islands with diameters larger than $\sim$20 nm account for over 45% of the total number of islands. The surface morphology difference suggests that the surface migration of In, Ga and As atoms is facilitated under an As-rich condition. For samples $QD_{In\text{-}only}$ and QD_{In+8s}, In(Ga)As QDs were formed mainly through the diffusion of As and Ga atoms from areas in the vicinity of the In droplets. This means that the spatial distribution of these QDs is mainly determined by the initial location of In droplets, and the In atoms did not migrate freely. For sample QD_{InAs}, the initial spatial distribution of In droplets should be similar to that in samples $QD_{In\text{-}only}$ and QD_{In+8s}. However, the presence of AsH_3 during the 8 s island crystallization significantly influenced the migration of In atoms, which then changed the size and island density. It has been reported that the hydrogen radicals stemming from AsH_3 decomposition during the MOCVD growth are very reactive and can attack the already formed InAs islands by breaking the In-As bonds.[33] This will lead to the "decomposition" of some small islands formed during the deposition of In droplets. The In atoms freed from the "decomposed" islands can migrate on the surface and find the most energetically favoured sites (e.g., the top of the islands) to sit and bind with As. This results in the formation of large In(Ga)As islands with a lower density.

Based on our experimental observations, a modified growth mechanism for the droplet epitaxy of In(Ga)As/GaAs is proposed, as summarised in Figure 4. In our case, In atoms were first deposited on the GaAs substrate surface as shown in Figure 4(a). However, the deposition of In droplets is immediately accompanied by an alloying process that results from As transport to the droplets as well as Ga diffusion from the substrate to the droplets (see Figure 4(b)), leading to the formation of $In_xGa_{1-x}As$. Following the supply of AsH_3 flow, further diffusion/migration of Ga and As atoms from the substrate is suppressed, while the surface migration of In and Ga under the presence of atomic hydrogen is enhanced, leading to the formation of large In(Ga)As islands with a low island density (Figures 4(c) and 4(d)).

In conclusion, we have investigated the growth mechanism of In(Ga)As QDs formed by droplet epitaxy. The unexpected mass transport of As and Ga from the GaAs substrate

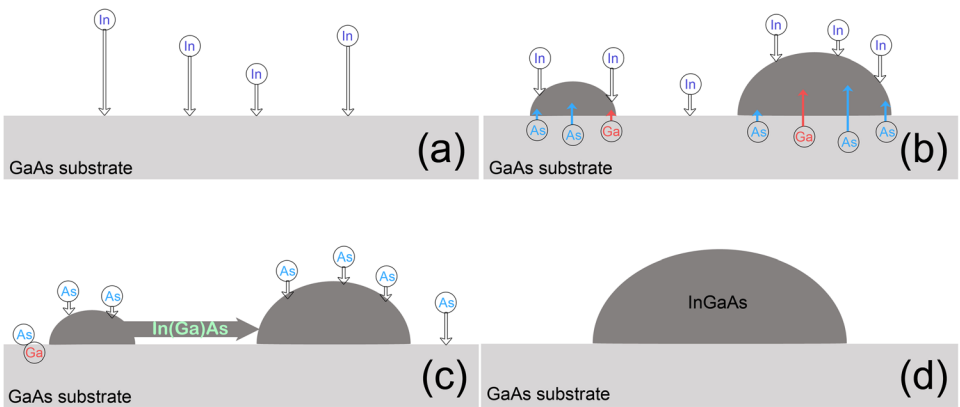

FIG. 4. Schematic illustration of the modified droplet epitaxy growth process.

into the In droplets was observed during the deposition stage of the droplets. This subsequently led to the crystallization of the droplets to form InGaAs QDs. The introduction of As flux after the droplet deposition step suppressed further diffusion of Ga and As from the substrate to the droplets. However, the presence of H radicals (from the dissociation of AsH_3) resulted in Ostwald ripening of the dots. These findings suggest that the mechanism for droplet epitaxy using MOCVD is somewhat different to that of Molecular Beam Epitaxy.[34]

The authors are grateful for the scientific and technical support from the Australian Microscopy and Microanalysis Research Facility node at the University of Sydney. We thank the Australian National Fabrication Facility for providing access to growth facilities used in this work. This research was financially supported by the Australian Research Council.

[1]H. Jiang and J. Singh, Phys. Rev. B **56**, 4696 (1997).
[2]J. Sabarinathan, P. Bhattacharya, P.-C. Yu, S. Krishna, J. Cheng, and D. G. Steel, Appl. Phys. Lett. **81**, 3876 (2002).
[3]A. Imamoglu, D. D. Awschalom, G. Burkard, D. P. DiVincenzo, D. Loss, M. Sherwin, and A. Small, Phys. Rev. Lett. **83**, 4202 (1999).
[4]E. Cohen, S. Yochelis, O. Westreich, S. Shusterman, and D. P. Kumah, Appl. Phys. Lett. **98**, 243115 (2011).
[5]A. Nemcsics, L. Toth, L. Dobos, Ch. Heyn, A. Stemmann, A. Schramm, H. Welsch, and W. Hansen, Superlattices Microstruct. **48**, 351 (2010).
[6]I. N. Stranski and L. Krastanow, Sitzungsber. Akad. Wiss. Wien, Math.-Naturwiss. Kl., Abt. 2A **146**, 797 (1937).
[7]N. Koguchi, K. Ishige, and S. Takahashi, J. Vac. Sci. Technol. B **11**, 787 (1993).
[8]I. Amlani, A. O. Orlov, G. Toth, G. H. Bernstein, C. S. Lent, and G. L. Snider, Science **284**, 289 (1999).
[9]G. Burkard, D. Loss, and D. P. DiVincenzo, Phys. Rev. B **59**, 2070 (1999).
[10]I. Kegel, T. H. Metzger, A. Lorke, J. Peisl, J. Stangl, G. Bauer, J. M. Garcia, and P. M. Petroff, Phys. Rev. Lett. **85**, 1694 (2000).
[11]A. Lemaitre, G. Patriarche, and F. Glas, Appl. Phys. Lett. **85**, 3717 (2004).
[12]X. Z. Liao, J. Zou, D. J. H. Cockayne, J. Qin, Z. M. Jiang, X. Wang, and R. Leon, Phys. Rev. B **60**, 15608 (1999).
[13]X. Z. Liao, J. Zou, D. J. H. Cockayne, R. Leon, and C. Lobo, Phys. Rev. Lett. **82**, 5148 (1999).
[14]X. Z. Liao, J. Zou, D. J. H. Cockayne, Z. M. Jiang, X. Wang, and R. Leon, Appl. Phys. Lett. **77**, 1304 (2000).
[15]X. Z. Liao, Y. T. Zhu, Y. M. Qiu, D. Uhl, and H. F. Xu, Appl. Phys. Lett. **84**, 511 (2004).
[16]J. Stangl, A. Hesse, V. Holy, Z. Zhong, G. Bauer, U. Denker, and O. G. Schmidt, Appl. Phys. Lett. **82**, 2251 (2003).
[17]J. H. Lee, K. Sablon, Zh. M. Wang, and G. J. Salamo, J. Appl. Phys. **103**, 054301 (2008).
[18]J. H. Lee, Zh. M. Wang, N. W. Strom, Yu. I. Mazur, and G. J. Salamo, Appl. Phys. Lett. **89**, 202101 (2006).
[19]R. Timm, H. Eisele, A. Lenz, L. Ivanova, G. Balakrishnan, D. L. Huffaker, and M. Dahne, Phys. Rev. Lett. **101**, 256101 (2008).
[20]Z. B. Chen, W. Lei, B. Chen, Y. B. Wang, X. Z. Liao, J. Zou, S. P. Ringer, and C. Jagadish, Scr. Mater. **69**, 638 (2013).
[21]D. Golberg, M. Mitome, L. W. Yin, and Y. Bando, Chem. Phys. Lett. **416**, 321 (2005).
[22]X. L. Li, J. Phys. Chem. C **114**, 15343 (2010).
[23]J. H. Lee, Z. M. Wang, and G. J. Salamo, IEEE Trans. Nanotechnol. **8**, 431 (2009).
[24]B. K. Chakraverty and R. W. Dreyfus, J. Appl. Phys. **37**, 631 (1966).
[25]E. Cohen, N. Elfassy, G. Koplovitz, S. Yochelis, S. Shusterman, D. P. Kumah, Y. Yacoby, R. Clarke, and Y. Paltiel, Sensors **11**, 10624 (2011).
[26]J. H. Lee, Z. M. Wang, M. E. Ware, K. C. Wijesundara, M. Garrido, E. A. Stinaff, and G. J. Salamo, Cryst. Growth Des. **8**, 1945 (2008).
[27]M. Malouin, F. El-Mellouhi, and N. Mousseau, Phys. Rev. B **76**, 045211 (2007).
[28]N. Q. Thinh, I. P. Vorona, I. A. Buyanova, and W. M. Chen, Phys. Rev. B **70**, 121201 (2004).
[29]L. Vegard, Z. Phys. **5**, 17 (1921).
[30]A. Rosenauer, U. Fischer, D. Gerthsen, and A. Forster, Appl. Phys. Lett. **71**, 3868 (1997).
[31]A. Ohtake and M. Ozeki, Phys. Rev. B **65**, 155318 (2002).
[32]A. Garcia, C. M. Mateo, M. Defensor, A. Salvador, and H. K. Hui, J. Appl. Phys. **102**, 073526 (2007).
[33]F. Heinrichsdroff, A. Krost, K. Schatke, D. Bimberg, A. O. Kosogov, and P. Werner, Proc.-Electrochem. Soc. **98**, 164 (1998).
[34]N. Koguchi, S. Takahashi, and T. Chikyow, J. Cryst. Growth **111**, 688 (1991).